JACS
JOURNAL OF THE AMERICAN CHEMICAL SOCIETY

COMMUNICATION

pubs.acs.org/JACS

Steam Etched Porous Graphene Oxide Network for Chemical Sensing

Tae Hee Han,[†] Yi-Kai Huang,[†] Alvin T. L. Tan, Vinayak P. Dravid,* and Jiaxing Huang*

Department of Materials Science and Engineering, Northwestern University, Evanston, Illinois 60208, United States

Supporting Information

ABSTRACT: Oxidative etching of graphene flakes was observed to initiate from edges and the occasional defect sites in the basal plane, leading to reduced lateral size and a small number of etch pits. In contrast, etching of highly defective graphene oxide and its reduced form resulted in rapid homogeneous fracturing of the sheets into smaller pieces. On the basis of these observations, a slow and more controllable etching route was designed to produce nanoporous reduced graphene oxide sheets by hydrothermal steaming at 200 °C. The degree of etching and the concomitant porosity can be conveniently tuned by etching time. In contrast to nonporous reduced graphene oxide annealed at the same temperature, the steamed nanoporous graphene oxide exhibited nearly 2 orders of magnitude increase in the sensitivity and improved recovery time when used as chemiresistor sensor platform for NO_2 detection. The results underscore the efficacy of the highly distributed nanoporous network in the low temperature steam etched GO.

Graphene oxide (GO) is usually made by reacting graphite powders with strong oxidants and acids,[1,2] through which the graphene sheets are partially oxidized and derivatized with oxygen containing functional groups, which makes them readily exfoliated into single layers in water.[3−5] Recent high resolution transmission microscopy studies[6] have confirmed earlier hypothesis[7] that the basal plane of GO is made of distributed graphitic nano patches separated by highly oxidized domains. GO is rather unstable, and can undergo *disproportionation* reactions, which are often referred to as "reduction" under mild heating to yield reduced GO (r-GO) (chemically modified graphene) and carbonaceous gases.[8−10] During the reduction of GO, the graphitic domains grow in size to form a percolated network, leading to partial restoration of electrical conductivity.[11] However, the harsh chemical oxidation reaction and the loss of carbon atoms during reduction introduce carbon vacancies in the basal plane. Therefore, both GO and its r-GO products are quite defective in their basal planes. This is the primary reason that the electronic properties of r-GO are much degraded compared to pristine graphene. Considerable effort has been directed to develop new reduction or processing techniques to repair the defects for converting GO to as perfect graphene as possible.[3−5,11] However, much less has been done to alter or even enlarge the defects, which would not only bring knowledge of the chemical reactivity of GO and r-GO, but also result in novel types of graphene-based sheets.

The defective nature of GO and r-GO could render them very different chemical reactivity compared to graphene. For example, if graphene is mildly heated in air, combustion of carbon atoms would initiate from the edges given relatively smaller number of additional defect sites in the basal plane, then gradually shrinking the sheet before its complete disappearance.[12] However, for GO or r-GO, since they contain abundant defect sites distributed throughout the basal plane, gasification of carbon atoms would occur homogeneously across the full face of the sheet, leading to rapid fracturing into small pieces. Indeed, the different behaviors were confirmed by SEM observation. Figure 1 shows SEM images of a few-layer graphene flake (Figure 1a−c) and AFM images of a GO sheet (Figure 1d−f) before and after heating in air at 600 °C, respectively. The graphene sample was heated for 10 min, while the GO sheet was heated only for 4 min. It was found that GO sheets would completely disappear between 4 and 5 min. Therefore, the GO sample was removed from the furnace just a moment before their complete combustion for AFM observations. Etching pits were seen to be heterogeneously distributed on the few-layer graphene flake (Figure 1b) but appeared to be uniformly distributed on GO sheets (Figure 1e). Additional SEM images showing typical fracturing patterns of GO can be seen in Figure S1. Overlaying the contours of the samples before and after oxidation highlights their different etching behaviors. As shown in Figure 1c, in addition to the etching pits, the graphene flake indeed

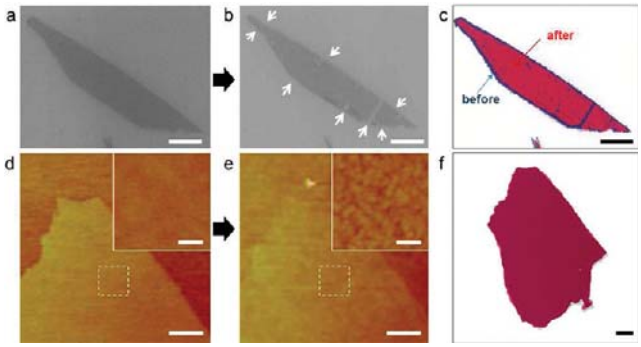

Figure 1. SEM and AFM images showing different modes of fracturing of (a−c) a few-layer graphene flake and (d−f) a GO sheet before their complete disappearance when heated in air at 600 °C. Etching pits and cracks were heterogeneously distributed on few-layer graphene flakes but appeared to be uniformly distributed on GO sheets in much greater number. All scale bars = 1 μm; scale bars in inset = 100 nm. (c and f) The contours of the sheets before and after oxidation were overlapped to highlight the change in size. For the graphene flake, size reduction suggests that etching started from the edges, which are more reactive. For GO, no apparent size reduction was observed, suggesting that edge sites are no more reactive than the defect sites in the basal plane.

Received: June 20, 2011
Published: September 06, 2011

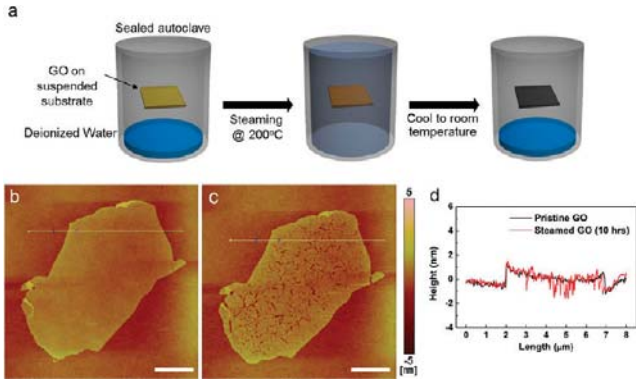

Figure 2. (a) Schematic drawings illustrating the steaming process to create perforated GO. First, GO monolayers were deposited on substrates by Langmuir−Blodgett technique. Then, the substrates were suspended above deionized water in the sealed vessel, and heated at 200 °C. (b and c) AFM images showing the same GO sheet before and after being steamed for 10 h, respectively. Pores and cracks can be clearly seen after steaming. (d) Height profiles along the white line in b and c. All scale bars = 2 μm.

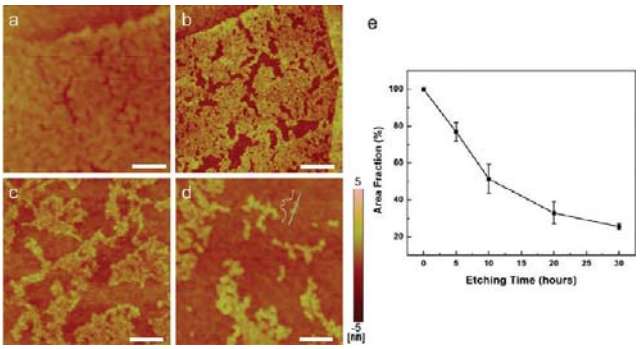

Figure 3. (a−d) Representative AFM images of GO sheets on Si wafer after streaming for 5, 10, 20, and 30 h, respectively. The initially continuous GO sheet first developed (a and b) pores and cracks, then turned into (c) a network of interconnecting nano-sized particles (around 20 nm), which finally broke into (d) isolated dots upon further steaming as indicated by height profile along white line. All scale bars = 200 nm. (e) The rate of etching as indicated by the change of area fraction of GO sheets after different steaming time.

shrank, suggesting that oxidation was faster at the edges. For GO (Figure 1f), no apparent size reduction was observed at this stage, suggesting that edge sites may even be less active than the defect sites in the basal plane. A recent report also showed that a GO sheet can rapidly break down to small pieces of around 10 nm in dimension upon oxygen plasma treatment for a few seconds.[13]

Although porous graphene has been made by lithography using block copolymer patterns[14,15] as mask, experiments shown in Figure 1 suggest that GO or r-GO should be a natural precursor to porous network of graphene-based materials, if opening of the defective sites can be better tuned to avoid mechanical breakdown. To achieve this, a milder and slower etching method is needed for better control over the progress of the oxidizing reactions. Here, we report that a porous graphene-based network can be conveniently synthesized by hydrothermal steaming of GO sheets with water. The resulting nanoporous graphene-based network showed significantly enhanced sensitivity toward chemical vapors.

Coal gasification[16] has been long studied for converting solid-state carbon-based materials to gaseous fuels such as CO and H_2 through the so-called water gas reactions with hot steam. Therefore, steaming GO sheets could also trigger the removal of carbon atoms,[17,18] likely to initiate from the more defective sp^3 rich domains. While typical water gas shift reactions require much higher temperature (>300 °C) treatment steps and the use of catalysts, we have discovered that steam etching of GO can occur at temperatures as low as 200 °C. The experimental setup is shown in Figure 2a. First, GO single layers were coated on SiO_2/Si substrates using Langmuir−Blodgett (LB) technique.[19] Then, each substrate was fixed at the neck of a glass pipet before putting it into a Teflon vessel prefilled with 10 vol % DI water. The substrates were suspended well above the water level to avoid direct wetting. The vessel was then sealed in a stainless steel autoclave and heated to 200 °C.

AFM was employed to examine the morphology of a single GO sheet before and after steam treatment. As shown in Figure 2b,c, after 10 h of streaming, many cracks were developed throughout the sheet. It is worth noting that no apparent size reduction was observed, and the cracks do not appear to be initiated from the edges. This fracturing behavior is similar to what was observed when heating GO in air (Figure 1d−f). Therefore, the edges of GO sheets do not appear to be the more reactive sites under steam etching conditions. Height profiles (Figure 2d) along the white lines in Figure 2b,c show that steamed GO was much roughened with many etched pits. The AFM line scan across the visible cracks reveals that GO was etched down through to the bottom substrate.

Since the basal plane of GO is a single atomic carbon layer, it is important to have a relatively slow etching reaction to allow sufficient time for controlling the porosity. In fast reactions such as direct heating in air or oxygen plasma treatment, GO is often broken down into discontinuous pieces within minutes or even seconds. Since the steaming temperature (200 °C) used here is rather low compared to the conventional water gas reactions, the degree of etching and the porosity of the resulting network can be conveniently controlled by exposure time. Figure 3a−d shows typical AFM images of the morphological evolution of GO sheets after steaming for 5, 10, 20, and 30 h, respectively. After 5 h of steaming (Figure 3a), the originally smooth GO surface started to appear particulate with particle size of around 20 nm. Some narrow cracks of around ∼20 nm wide can already be observed. After 10 h of steaming (Figure 3b), much larger cracks with nominal width of around 100 nm can be seen, and a more open network of interconnecting particulate domains was formed. Further etching (20−30 h) continued to reduce the coverage of materials, leading to a much less dense network (Figure 3c), and eventually broke the continuity of the network (Figure 3d). Figure 3e shows the change of coverage within the initially continuous GO sheets as a function of steaming time. Since graphitic carbon atoms are less reactive, as steaming time increases, the fraction of graphitic domains in GO should increase due to an annealing effect at 200 °C and the preferential removal of sp^3 regions in the early stage of the reaction. Therefore, the etching reaction rate was relatively slower in the later stage of etching (>10 h).

Because of its limited lateral resolution, AFM study does not reveal the detailed structures of the roughened GO sheets during initial etching (Figure 3a). To examine the effect of steaming with TEM, free-standing GO sheets were deposited on lacey carbon

dx.doi.org/10.1021/ja205693t | J. Am. Chem. Soc. 2011, 133, 15264–15267

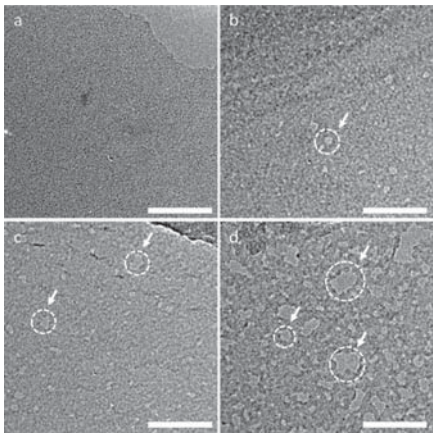

Figure 4. TEM images of freely suspended GO sheets (a) before and after being steamed for (b) 5, (c) 10, and (d) 20 h. After 5 h steaming, many pores of a few nanometers in diameter were already developed. Further etching results in more and larger pores. The white circles in the images highlight a few pores. All scale bars = 50 nm.

coated copper grids and then subjected to steam treatment. Although the etching rates on the free-standing GO sheets supported on copper grid may be different than those of SiO_2/Si supported GO, TEM observation can still provide useful information regarding the early stage of etching. Figure 4a−d shows TEM images of GO before and after 5, 10, 20 h of steam treatment, respectively. After 5 h of steaming (Figure 4b), there were already many holes which appeared on the GO sheets with broadly distributed diameters ranging from approximately 2 to 40 nm. Longer steaming time (Figure 4c,d) resulted in a more porous GO membrane with a greater number of pores of increasing sizes. Additional low magnification TEM images are included in Figure S2. Therefore, TEM study confirmed that steaming with water vapor is indeed an effective way to open nanoscale pores on GO and convert it into a nanoporous network.

We hypothesize that the etching mechanism under steaming is analogous to coal gasification, where carbon atoms react with H_2O vapor to produce CO and H_2, leaving behind carbon vacancies that eventually grow into large pores.[16−18] To confirm the role of water vapor in etching, several control experiments were carried out to heat GO in the autoclave at 200 °C without water, or with several different solvents for 20 h. Figure S3 shows the typical AFM images of such treated GO. As shown in Figure S3a, dry heating did not result in detectable etching of GO by AFM. Similarly, steaming GO with toluene (Figure S3b) or ethanol (Figure S3c) did not produce porous or fractured sheets either. In separate experiments, adding an oxidative compound such as H_2O_2 into water (1%) was found to greatly accelerate the etching process. Therefore, we conclude that water vapor acts as a mild etchant for carbon atoms during steaming. As is with oxidation in air (Figure 1b), etching by steam should also start from the relatively more reactive sp^3 carbon sites, which are distributed throughout the basal plane of GO. This leads to distributed pores all over the sheet, eventually forming the porous network. In a control experiment, GO sheets were first reduced by either thermal annealing or hydrazine treatment, and then subjected to steaming. As shown in Figure S4a-S4d, steaming had the same etching effects on r-GO, but etching proceeded much more slowly. This is consistent with the more

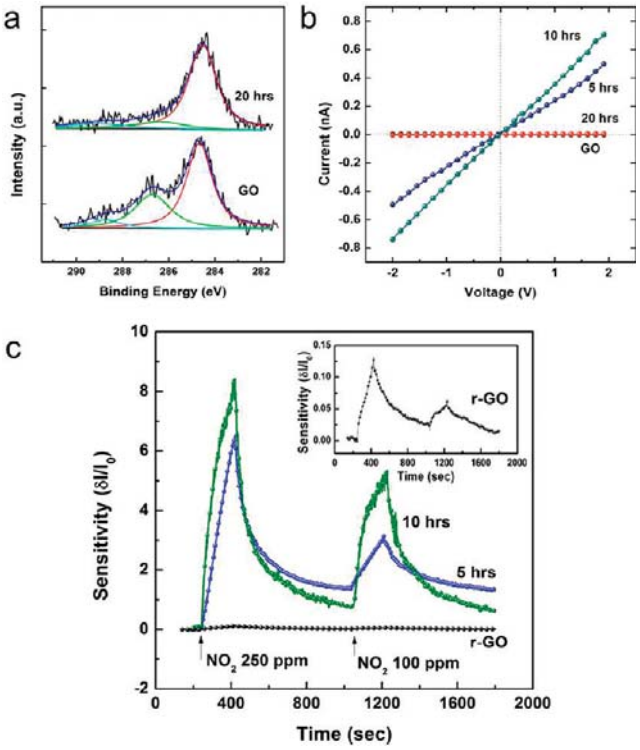

Figure 5. (a) XPS spectra of GO monolayer before and after being steamed for 20 h, suggesting that GO has undergone deoxygenation after steaming. (b) I−V curves of pristine GO and steamed GO samples. Even though GO sheets become porous after steaming, their conductivity still increases (5 and 10 h) before breaking into a nonpercolated network (20 h). This suggests that GO sheets were also reduced during steaming. (c) Responses of thermally reduced r-GO and the steamed GO sheets upon exposure to NO_2 vapor. Sensitivity increases with steaming time, likely due to the increased edge fraction and porous nature of steamed samples.

graphitic nature of r-GO, which renders it more robust against oxidation. However, r-GO is still quite defective, leading to similar morphology of the final etched sheets.

Since GO can undergo the deoxygenation reaction at around 150 °C,[9] while being steamed at 200 °C, GO can still be partially reduced. Figure 5a shows the XPS spectra of GO before and after 20 h steaming. The band at around 287 eV corresponding to the oxygenated carbon functional groups is much reduced after steaming, suggesting that steamed GO has undergone deoxygenation. Therefore, the steamed GO should become electrically conductive even if it is etched into a porous but percolated network. Figure 5b shows the I−V curves of GO monolayers before and after steaming for 5, 10, and 20 h. Increased current was indeed observed for GO steamed for 5 and 10 h. The samples steamed for 20 h were often found to be insulating due to over-etching that breaks the percolating network (Figure 3d).

r-GO has attracted significant interest as a material for gas sensing applications.[20−25] Prior work on single walled carbon nanotubes revealed that their oxygenated defect sites (i.e., −COOH) have stronger interaction with the gas molecules, therefore dominating the overall sensing response.[26] The steamed GO has a porous network structure with abundant edge sites, which should be terminated with oxygenated groups through reaction with water vapor. To test whether steamed GO has enhanced interaction with

gas molecules, chemiresistors were fabricated using the porous r-GO network as the sensing material. NO_2 is a toxic pollutant produced from various combustion processes and has been intensively investigated as a model system for graphene based gas sensors;[21−25] therefore, it is chosen here to test the effect of steam etching on r-GO's sensing performance. Figure 5c shows the response of regular r-GO and porous r-GO after 5 and 10 h of steaming treatment on exposure to NO_2 vapor. The r-GO control sample was prepared by annealing at 200 °C. All the 3 samples showed increased current on exposure to NO_2, which is consistent with the *p*-type nature of r-GO.[21−25] The sensitivity of regular, nonporous r-GO was comparable to some previously reported r-GO NO_2 sensors.[23,24] For steamed GO, however, nearly 2 orders of magnitude of higher sensitivity was observed, and longer steam treatment led to higher sensitivity, likely due to higher porosity (Figures 3 and 4). Devices made with r-GO samples after 20 h of steaming had very low successful yield since the r-GO network was largely broken (Figure 3d). The recovery time of the sample steamed for longer time was also more rapid, which can be attributed to higher joule heating effect due to the higher current (Figure 5b).

In summary, hydrothermal steaming of GO creates an electrically conductive, nanoporous r-GO network. Compared to regular r-GO, the porous r-GO shows greatly improved performance as gas sensor for NO_2. Since r-GO itself is already a quite defective structure with sp^3 carbon atoms in the basal plane, the much enhanced sensitivity with porous r-GO suggests that interaction between NO_2 molecules and the edge defects produce more pronounced changes in current. The ease of fabrication and enhanced interaction with gas molecules could make porous r-GO a general and effective platform for designing high performance sensors or gas storage materials.

■ ASSOCIATED CONTENT

Ⓢ Supporting Information. Experimental details and other supplementary data. This material is available free of charge via the Internet at http://pubs.acs.org.

■ AUTHOR INFORMATION

Corresponding Author

v-dravid@northwestern.edu; Jiaxing-huang@northwestern.edu

Author Contributions

[†]These authors contributed equally.

■ ACKNOWLEDGMENT

This work was supported by the National Science Foundation through DMR CAREER 0955612, ECCS 925882 and the NSF-NSEC program at Northwestern University (EEC 0647560). Additional support was provided by the Northrop Grumman Corporation and the Sony Corporation. A.T.L.T. thanks the Defense Science and Technology Agency of Singapore for an overseas undergraduate scholarship. J.H. is an Alfred P. Sloan Research Fellow. Microscopy and surface analysis were carried out at the NU*ANCE* center at Northwestern University.

■ REFERENCES

(1) Brodie, B. C. *Philos. Trans. R. Soc. London* **1859**, *149*, 249.
(2) Hummers, W. S.; Offeman, R. E. *J. Am. Chem. Soc.* **1958**, *80*, 1339.
(3) Li, D.; Kaner, R. B. *Science* **2008**, *320*, 1170.
(4) Park, S.; Ruoff, R. S. *Nat. Nanotechnol.* **2009**, *4*, 217.
(5) Compton, O. C.; Nguyen, S. T. *Small* **2010**, *6*, 711.
(6) Erickson, K.; Erni, R.; Lee, Z.; Alem, N.; Gannett, W.; Zettl, A. *Adv. Mater.* **2010**, *22*, 4467.
(7) Lerf, A.; He, H. Y.; Forster, M.; Klinowski, J. *J. Phys. Chem. B* **1998**, *102*, 4477.
(8) Croft, R. C. *Q. Rev. Chem. Soc.* **1960**, *14*, 1.
(9) Kim, F.; Luo, J.; Cruz-Silva, R.; Cote, L. C.; Sohn, K.; Huang, J. *Adv. Funct. Mater.* **2010**, *20*, 2867.
(10) Schniepp, H. C.; Li, J. L.; McAllister, M. J.; Sai, H.; Herrera-Alonso, M.; Adamson, D. H.; Prud'homme, R. K.; Car, R.; Saville, D. A.; Aksay, I. A. *J. Phys. Chem. B* **2006**, *110*, 8535.
(11) Mattevi, C.; Eda, G.; Agnoli, S.; Miller, S.; Mkhoyan, K. A.; Celik, O.; Mostrogiovanni, D.; Granozzi, G.; Garfunkel, E.; Chhowalla, M. *Adv. Funct. Mater.* **2009**, *19*, 2577.
(12) Brus, L. E.; Liu, L.; Ryu, S. M.; Tomasik, M. R.; Stolyarova, E.; Jung, N.; Hybertsen, M. S.; Steigerwald, M. L.; Flynn, G. W. *Nano Lett.* **2008**, *8*, 1965.
(13) Solis-Fernandez, P.; Paredes, J. I.; Villar-Rodil, S.; Guardia, L.; Fernandez-Merino, M. J.; Dobrik, G.; Biro, L. P.; Martinez-Alonso, A.; Tascon, J. M. D. *J. Phys. Chem. C* **2011**, *115*, 7956.
(14) Kim, M.; Safron, N. S.; Han, E.; Arnold, M. S.; Gopalan, P. *Nano Lett.* **2010**, *10*, 1125.
(15) Bai, J. W.; Zhong, X.; Jiang, S.; Huang, Y.; Duan, X. F. *Nat. Nanotechnol.* **2010**, *5*, 190.
(16) Smoot, L. D.; Smith, P. J. *Coal Combustion and Gasification*; Plenum Press: New York, 1985.
(17) Yang, R. T.; Yang, K. L. *Carbon* **1985**, *23*, 537.
(18) Necatioz., M; Nordwall, H. J. *Nucl. Sci. Eng.* **1971**, *44*, 310.
(19) Cote, L. J.; Kim, F.; Huang, J. X. *J. Am. Chem. Soc.* **2009**, *131*, 1043.
(20) Robinson, J. T.; Perkins, F. K.; Snow, E. S.; Wei, Z. Q.; Sheehan, P. E. *Nano Lett.* **2008**, *8*, 3137.
(21) Fowler, J. D.; Allen, M. J.; Tung, V. C.; Yang, Y.; Kaner, R. B.; Weiller, B. H. *ACS Nano* **2009**, *3*, 301.
(22) Lu, G. H.; Ocola, L. E.; Chen, J. H. *Appl. Phys. Lett.* **2009**, *94*, 083111.
(23) Dua, V.; Surwade, S. P.; Ammu, S.; Agnihotra, S. R.; Jain, S.; Roberts, K. E.; Park, S.; Ruoff, R. S.; Manohar, S. K. *Angew. Chem., Int. Ed.* **2010**, *49*, 2154.
(24) Jeong, H. Y.; Lee, D. S.; Choi, H. K.; Lee, D. H.; Kim, J. E.; Lee, J. Y.; Lee, W. J.; Kim, S. O.; Choi, S. Y. *Appl. Phys. Lett.* **2010**, *96*, 213105.
(25) Lu, G. H.; Park, S.; Yu, K. H.; Ruoff, R. S.; Ocola, L. E.; Rosenmann, D.; Chen, J. H. *ACS Nano* **2011**, *5*, 1154.
(26) Robinson, J. A.; Snow, E. S.; Badescu, S. C.; Reinecke, T. L.; Perkins, F. K. *Nano Lett.* **2006**, *6*, 1747.